First-principles studies of hydrogen interaction with ultrathin Mg and Mg-based alloy films

Mina Yoon, Hanno H. Weitering, and Zhenyu Zhang

First-Principles Theoretical Studies of Hydrogen Interaction

with Ultrathin Mg and Mg-based Alloy Films

Mina Yoon,[1,2] Hanno H. Weitering, [3,1] Zhenyu Zhang[1,3,4]

[1]*Materials Science and Technology Division, Oak Ridge National Laboratory, Oak Ridge, TN 37831*

[2]*Fritz-Haber-Institut der Max-Planck-Gesellschaft, Faradayweg 4-6, 14195 Berlin, Germany*

[3]*Department of Physics and Astronomy, The University of Tennessee, Knoxville, TN 37996*

[4]*ICQD, University of Science and Technology of China, Hefei, Anhui, 230026, China*

ABSTRACT

The search for technologically and economically viable storage solutions for hydrogen fuel would greatly benefit from research strategies that involve systematic property tuning of potential storage materials via atomic-level modification. Here, we use first-principles density functional theory (DFT) to theoretically investigate the structural and electronic properties of ultrathin Mg films and Mg-based alloy films and their interaction with atomic hydrogen. Additional delocalized charges are distributed over the Mg films upon alloying them with 11.1% of Al or Na atoms. These extra charges contribute to enhance the hydrogen binding strength to the films. We calculated the chemical potential of hydrogen in Mg films for different dopant species and film thickness, and included the vibrational degrees of freedom. By comparing the chemical potential with that of free hydrogen gas at finite temperature (T) and pressure (P), we construct a hydrogenation phase diagram and identify the conditions for hydrogen absorption/desorption. The formation enthalpies of metal hydrides are greatly increased in thin films, and in stark contrast to its bulk phase, the hydride state can only be stabilized at high P and T (where chemical potential of free H_2 is very high). Metal-doping increases the thermodynamic stabilities of the hydride films and thus significantly helps to reduce the required pressure condition for hydrogen absorption from H_2 gas. In particular, with Na alloying hydrogen can be absorbed/desorbed at experimentally accessible T and P conditions.

PACS numbers: 68.43.Bc, 68.90.+g, 81.05.Zx, 84.60.Ve

I. INTRODUCTION

Hydrogen has been viewed as a highly appealing energy carrier for renewable energy applications because of its abundance and environmental friendliness [1]. To achieve economic feasibility, hydrogen storage materials with high gravimetric and volumetric densities must be developed [2]. Furthermore, hydrogen recycling should be performed reversibly under near ambient conditions [2].

Metal hydrides are interesting materials for hydrogen storage due to their high hydrogen storage capacity and structural stability. In many hydrides the hydrogen density is even higher than in liquid hydrogen [3]. Among all metal hydrides that have been studied so far, Magnesium hydrides are promising materials with a high hydrogen gravimetric density (7.7 wt%), while being a low cost material. However, serious issues need to be resolved; 1) the high thermodynamic stability of Mg hydrides implies slow hydrogen kinetics. 2) Their high reactivity toward air or oxygen is problematic. To reduce the kinetic barriers for hydrogen absorption and desorption, one must somehow destabilize the Mg hydride. Such a destabilization can be induced by introducing chemical or structural modifications. Previous studies have shown that the formation enthalpies of hydrides can be higher by adding other elements to the system [4], thus hydrogen desorption temperatures are lower. However, the temperature for releasing hydrogen still remains far above the requirements for ambient condition applications. Moreover, a major drawback of this approach is that it is accompanied by a significant reduction of the storage capacity [5]. Recent studies have shown that hydrogen adsorbed on nanostructured Mg can be released at a low temperature and it can be even significantly lowered if other compounds such as carbon nanotubes are added to the material [6].

Thin metal (hybrid) films are an interesting storage medium because they exhibit large surface to volume ratios and facilitate fast hydrogen diffusion. It is comparably easy to chemically modify these systems. Ultrathin metal films are very intriguing materials, because their chemical properties can be modified interactively by changing the thickness of the films as a result of quantum size effects [7,8]. Moreover, the low structural stabilities of ultrathin Mg films may help to reduce the required temperature for releasing absorbsed hydrogen to the system. Thin Mg films have already been synthesized on various substrates [9-11]. Recent

studies have shown that the hydrogen affinity of the system can be carefully modulated by changing the thickness of the Mg film [12].

In this paper, we theoretically study the fundamental properties of ultrathin Mg and Mg-based alloy films and their interaction with atomic hydrogen using DFT. Additional delocalized charges are distributed over the Mg films upon alloying them with 11.1% of Al or Na atoms. These extra charges contribute to enhance hydrogen binding strength to the films. Within harmonic approximations we calculate the Gibbs free energy of the structures by including all available phonon modes and zero point energy at a given temperature. By comparing structural stabilities of hydrogenated and non-hydrogenated structures, we construct hydrogenation phase diagrams in temperature (T) and pressure (P) space, and identify the conditions for hydrogen absorption/desorption. The formation enthalpies of metal hydrides are greatly increased in thin films, and in stark contrast to its bulk phase, the hydride state can only be stabilized at high P and T (where chemical potential of free H_2 is very high). Metal doping increases the thermodynamic stability and significantly helps reduce the required pressure condition for hydrogen absorption from H_2 gas. In particular, with Na doping hydrogen can be reversibly adsorbed at experimentally accessible T and P conditions.

The paper is organized as follows. In Sec.II we explain our theoretical approaches and model structures. Structural properties of Mg and alloyed films are discussed in Sec.III. In Sec.IV our model structures for hydrogenated Mg and alloyed films and hydrogen affinity to different films will be discussed. In Sec. V we discuss thermodynamic properties of ultrathin Mg and Mg-based alloy films and hydrogenated films. We will summarize in Sec. VI.

II. THEORETICAL MODELLING

Our total energies are obtained from DFT with an all electron full potential scheme and a numerical atom-centered orbitals (NAO) basis as implemented in the FHI-aims code [13]. We employed "tight" setting including the standard NAO basis set "tier1" for Mg, Na, and Al and "tier2" for H [13, 14]. This choice of basis settings leads to a converged hydrogen binding energy to films to be changed on the scale of meV with respect to the number of basis functions. The exchange correlation potential of Perdew-Burke-Ernzerhof (PBE) version of the generalized gradient approximation (GGA) [15] was used and also compared with local-density

approximations (LDA) [16]. We modelled pristine Mg films as 1x1 supercells with thickness (τ) of 2 to 8 ML stacked along the (0001) direction of the hexagonal close-packed (hcp) structure. In our approach, there is no significant computational cost for calculating the structure with a large vacuum layer, thus we adopted a sufficiently large vacuum layer of 70.0Å. For alloys, 3x3 supercells with thickness of 2 to 5 ML were considered and 1/9 of Mg atoms in each layer were replaced by either Al or Na, which becomes Al_xMg_{1-x} or Na_xMg_{1-x} with x=1/9. The supercell calculations were performed using k-point mesh points 5x5x1 for the metal slabs and 15x15x15 meshes for bulk metal.

III. STRUCTURAL PROPERTIES OF ULTRATHIN MG AND ALLOYED FILMS

Magnesium forms hcp as a stable crystal structure at ambient conditions. We obtained lattice constants of a=3.209Å and c=5.188 Å by fitting a series of total energies to the Birch-Murnaghan [17] equation of states for finding the optimum c/a ratio for a given lattice parameter a, then a fourth order polynomial function was employed to determine an optimum lattice constants a and c [18]. These values compare well with experimental values of a=3.21 Å and c=5.21 Å [19]. The equilibrium phase of Mg is close to the ideal hcp close-packing value of $c/a= \sqrt{8/3} \approx 1.633$; this phase remains stable up to a high pressure, since Mg is a very compressible metal with bulk modulus of 35.4 GPa [19]. At high temperatures and pressures, a structural transformation from hcp to body-centered cubic (bcc) phase (through dhcp (double hexagonal close-packed transition)) was observed experimentally [20].

Ultrathin Mg films have been synthesized in (0001) direction on different types of substrates such as Al(111) [9], Mo(111) [10], and Pd [11]. Electronic band structure calculations along the Mg (0001) direction show that the Fermi wave vector spans 23% of the distance between Γ and A, suggesting that the structural stability of (0001) oriented films oscillates as a function of thickness. Specifically, a 25% distance corresponds to an oscillation period of 8 monolayers (ML) [8,12]. This oscillating behaviour can be attributed to quantum size effects [21].

We determined the optimum lattice parameters (a and c) of each film (where all the layers are equidistant) by fitting a series of total energy data to the Birch-Murnaghan equation of states and polynomial functions as discussed above. Then, atoms are fully relaxed in order to further optimize interlayer spacings within an optimized cell. We maintain the hcp symmetry of the

optimized cell during the relaxation processes. The equilibrium lattice constants for bulk alloys are a=3.1 Å, c=5.0 Å for Al_xMg_{1-x} and a=3.3 Å, c=5.3 Å for Na_xMg_{1-x}, where x=1/9. These values correspond to changes of the lattice constants by -2.8% for a and -3.8% for c for the Al case and +3.4% for a and +1.9% for c for the Na case. This trend holds also for the films as illustrated with the distance distribution function (distance distribution function, DDF) in Fig. 1 (**a**), where the blue, red, and green lines represent the cases of Mg, NaMg, and AlMg films respectively and each graph represents a different film thickness (τ). The first peaks correspond to the first-nearest-neighbour distances between the Mg atoms as well as between Mg atoms and metal dopants. The average nearest neighbor distance between the Mg atoms is ≈3.1 Å; the average -Al-Mg and Na-Mg distances are ≈3.0 Å and ≈3.3 Å for AlMg and NaMg, respectively. Hence, the average interatomic -distances in the (a,b) plane are ≈1.5% shorter (longer) for AlMg (NaMg), compared to pure Mg. We also observe a significant displacement of metal dopants at the surface lattice locations; the Na atoms move outward and their distance to the second neighbours (i.e. atoms in the next layer) increases to ≈3.8 Å. In the case of AlMg, Al atoms at the surface relax inward and the second neighbour distance becomes ≈3.1Å. As we will show, the expansion of the interlayer spacing near the Na dopants helps to accommodate hydrogen atoms.

IV. THERMODYNAMIC PROPERTIES OF MG AND ALLOYED FILM HYDRIDES

A. Structural Properties

The hydrogen atoms were initially positioned at the fcc site in the middle of two ML of 1x1 films (bulk site). These units are repeated for thicker films and alloys. We determined the optimum lattice parameters of a and c (where all the layers are equi-distant) for hydrides by fitting a series of total energy data in a and c spaces into the Birch-Murnaghan equation of states and polynomial functions. Then, we performed a full optimization of atomic positions for a given optimized cell, where all the interlayer spacing as well as hydrogen positions are fully relaxed. The distance distribution functions of the hydrides are shown in Fig. 1(**b**). The distributions below ≈2.8Å arise only from the bonding between H and Mg and between H and the metal

dopants. The distance distributions for H-Mg are similar for the Mg, AlMg, and NaMg films and the shortest distance peaked at ≈2.0 Å. However, the Al-H and Na-H distances in the respective alloy films are quite different. The shortest Al-H distances in the AlMg films average to ~1.8 Å (~2.0Å for τ=2ML). On the other hand, the Na-H distances in the NaMg films has a first peak at ≈2.3 Å (Due to the high density of Mg-H peaks in the DDF, the described trends are not visible in Fig.1(**b**)). High amount of charges is accumulated at the metal dopants. These extra charges contribute to a stronger Coulomb interaction between negatively charge H atoms and metal films. H atoms are homogeneously dispersed in AlMg (with a high density in DDF, peaked at ≈2.9Å) driven by Coulomb repulsion between Al and H. Negatively charged H atoms are closely located to the negatively charged Na atoms, which results in a high density of DDF at a shorter distance (≈2.3Å) (Due to the high density of Mg-H and Mg-Mg peaks in the DDF, the described trends are not visible in Fig.1(**b**)). The charge density profiles of each element will be discussed in the next session. The Mg-H distances in the Na and Al doped films are ≈2.0 Å, which is slightly shorter than those of pristine Mg films, where ≈2.1 Å for the Mg-H distances (for 2ML, the hydrogen atoms are located at the center of the slab, producing a peak at ≈2.3 Å). An interesting feature is that the interlayer spacings of the NaMg films do not change much with hydrogenation, because the interlayer spacings of films have already expanded (compared to pristine Mg) so that H can be easily accommodated. On the other hand, the already compressed AlMg interlayer spacing increases upon hydrogenation.

B. Charge density analysis

We have evaluated partial electron charges of each atom using the Hirshfeld analysis [22]. Figure 2 presents partial charge densities of individual species, Mg(**a**), Na or Al (**b**), and H (**c**) of fully relaxed geometries. These values are averaged over each element. The positive values correspond to the amount of accumulated electrons and the negative values for accumulated holes. The dotted lines with unfilled points denote for the data points of non-hydrided films (M(M=Na, Al)Mg) and solid lines with filled points for hydrided films (MMg-H). Upon Na alloying, excess electrons are accumulated to the Mg sites, and the average charge upto ≈0.01e. Electrons at Mg sites are depleted upon Al alloying with the amount less than 0.02e. These features can be seen in Fig. 2(**a**). These transferred charges are compensated by those at the dopant sites, i.e. a depletion of charges at Na sites (upto ≈0.1e) and accumulation of charges at

Al sites (upto ≈0.15e) (see Fig.2(**b**)). The amount transferred charges are higher in Mg sites of hydrided films. For all the hydrided films, excess electrons are depleted at Mg sites, which means that hydrogen is negatively charged. The charge states (δ) of hydrogen (H$^\delta$) ranges between ≈-0.13e and -0.17e, a smallest charge transfer for pristine Mg films and a largest charge transfer for Na-alloyed films. The hydrogen electron density can be related to the H embedding energy as discussed in the literatures [23-25]. We confirmed that there is a strong correlation of H partial densities to its binding strength to the metals. In particular, the hydrogen binding curve shown in Fig.3(**a**) follows the trends shown in Fig.2(**c**).

C. Vibrational energy and hydrogen affinity

We employed harmonic approximations [13] to evaluate the full vibrational spectra of the films. Within the harmonic approximation the vibrational free energy (F_{vib}) can be evaluated as

$$F_{vib} = \int d\omega\, g(\omega)[\hbar\omega/2 + k_B T \ln(1-\exp(-\hbar\omega/k_B T))], \quad (1)$$

where $g(\omega)$ is the phonon density of states of the optimized films. We take the all the vibrational modes contributing to all the degrees of freedom of atoms into account. For non-hydrogenated films the spectrum ranges from 0 to ≤400cm^{-1} (slightly larger ranges in the cases of NaMg and AlMg). Hydrogenation makes the related bonds very stiff, thus the overall eigenfrequencies extend up to ~ 1000cm^{-1} for alloys and ≈800cm^{-1} for Mg films. In particular, the characteristic frequencies of the hydrogen bonds lie above ≈400cm^{-1}.

Next, we investigated the interaction between atomic hydrogen and ultrathin films. The formation enthalpies of hydride films at T can be written as

$$\Delta H = (U + PV)_{H+film} - (U + PV)_{film} - N_H H_H \approx \Delta U_{film} - N_H H_H, \quad (2)$$

by assuming that changes in film volumes (V) from hydrogenation are negligible. Here U is the internal energy of the film including electronic part of total energy (E), phonon contribution to the internal energy, and zero point energy (ZPE). H_H is the formation enthalpy of hydrogen at T and N_H is the total number of hydrogen atoms. We considered dihydrogen (H$_2$) gas as reference systems and used experimental data [26] for formation enthalpy and total energy and zero point energy from our calculations. We obtained zero point energy of H$_2$ ≈0.27eV from GGA calculations, which is in excellent agreement with experimental value of 0.273eV [27].

Figure 3(**a**) presents the hydride formation enthalpies per hydrogen atom at T=0 (ΔH, solid lines) as a function of film thickness (τ). These values are compared to the enthalpies without inclusion of the vibrational contribution (ΔE, dashed lines). The metal-doped films become significantly stiffer upon introducing hydrogen. By comparing phonon density of states of Mg and metal-doped Mg films, we observe that metal-doped film hydrides have a much higher density of states at low frequency ($\omega<300cm^{-1}$) with some additional states at higher frequency. As a result, the formation enthalpies (ΔH) of the metal-doped films at T=0 are higher than the formation energies without vibrational contributions (ΔE) (see Fig.3(**a**)). Therefore, the ZPE contributions lower the hydrogen binding strength of metal-doped films, except for the AlMg film with τ=2 where the ZPE slightly increases the hydrogen binding energy ($\approx$0.02eV).

For pristine Mg films, the vibrational energy penalty in the hydride films is completely offset by the ZPE of free H_2. Consequently, the formation enthalpy is smaller than ΔE. The ZPE energy contribution in the H binding energy can be significant; The energy gain in the H binding strength from these vibrational contributions ranges from 0.13 to 0.02eV/H. On the other hand, ZPE of hydride films increases for alloys and ΔH becomes similar or slightly higher than ΔE. Na doping significantly increases the hydrogen affinity by up to $\approx$0.17eV/H. The NaMg film with τ=4 is the only film that can be hydrogenated from H_2 gas in thermodynamic equilibrium at T=0 and P=1bar, i.e. $\Delta H_{1/2H_2} < 0$. On the other hand, if the films are exposed to atomic H gas, all films can be hydrogenated, with formation enthalpies (ΔH_H) ranging from -2.2 to $\approx$-1.8 per H atom.

Fully hydrogenated bulk Mg forms rutile MgH_2. For the formation enthalpy of MgH_2 at T=0 we obtained -0.46eV from our GGA calculation, which is smaller than the experimental value of -0.706eV per H [27]. It is known that the calculations from PBE exchange-correlation functional underestimate enthalpies of alkaline earth hydrides, while LDA overestimates them [28]. The experimental value lies between the PBE and LDA values.

D. Hydrogen absorption/desorption phase diagram

The Gibbs free energy (G) is a measure for the structural stability of a system at a finite temperature and pressure (P). In particular, chemical potential differences ($\Delta\mu$) between different systems determine their relative structural stability. We evaluate the chemical potential of

hydrogen ($\Delta\mu_H$) in films with respect to that of free H_2 gas, which is described by the ideal gas equation [29];

$$\Delta\mu_H(T,P) = \left((E+F_{vib})_{H+film} - (E+F_{vib})_{film}\right)/N_H - 1/2\left[\mu_{H_2}^0 + E_{H2} + E_{H2}^{ZPE} + k_BT\ln(P/P_0)\right]. \quad (3)$$

Here we assume that changes in film volumes at a given P are negligible. E is total energy obtained from our DFT calculations, F_{vib} is vibrational free energy including zero point energy, E_{H2}^{ZPE} is zero point energy of H_2, 0.27eV from our PBE calculations. P_0 denotes 1 bar, k_B for Boltzmann constant, and $\mu_{H_2}^0$ for chemical potential of H_2 with reference to $T=0$ and $P=1$bar state, which is taken from the experimental value [26]. Figures 3 (**b**)-(**d**) show the chemical potential of hydrogen of different films as a function of T at $P=1$ bar, with respect to that of free H_2 gas. The calculations were performed for the structures with specific constraint, i.e. conservation of hcp symmetry and hydrogen atoms are located at fcc site as described in the previous sections. Therefore, configurational entropy, which may play an important role at a high temperature is not taken into account. In the figures different colors represent different film thicknesses (blue, red, green, and black solid lines for thickness 2, 3, 4, and 5 films, respectively). At $P=1$bar hydrogenation is an exothermic process only for the NaMg film with $\tau=4$ and $T < 100$K. This film contains 2.03wt% of hydrogen. The chemical potential differences increase linearly with temperature. We extract the pressure conditions satisfying $\Delta\mu_H = 0$, for a given temperature, to determine the phase boundary for reversible absorption and desorption. The hydrogenation phase diagrams are presented in Fig. 4. Each line identifies the boundary conditions for reversible hydrogen absorption and desorption; below each line hydrogen is desorbed whereas hydrogen adsorbs above the line. The chemical potentials of hydrogen in AlMg or Mg films (Fig. 3) at P=1bar are high with respect to that of free H_2, i.e. $\Delta\mu_H > 0$, which implies that hydrogen absorption is only possible for $P>1$bar regardless of the temperature range. In fact, for a given T, extremely high P is required for H absorption; for example $P \geq 10^7$ bar at room T (see Fig.4(**a**) and (**c**)). For a given $P(>>1$bar), hydrogen absorption is possible by increasing T so that the chemical potential of ideal H_2 gas (which is described by $\approx k_BT\ln(P/P_0)$) becomes higher than that of the absorbed hydrogen.

The Na-alloyed Mg film with $\tau=4$ is a special case, where chemical potential of hydrogen is lower than that of gas phase at $T=0$ (see Fig. 3(**a**)). Hydrogen absorption is possible for $P<1$bar and adsorbed hydrogen can be desorbed by increasing T at a given P. There, we can adsorb

hydrogen at experimentally accessible T and P conditions. For example, H-desorption/absorption reactions can occur near $T\approx200K$ and $P\approx67$ bar by slightly modifying either T or P values.

VI. SUMMARY AND DISCUSSION

We theoretically investigated the fundamental properties of properties of ultrathin Mg and Mg-based alloy films and their interaction with atomic hydrogen using first-principles density functional techniques. Introducing metal dopants to the films leads to distinctive changes in their structural and electronic properties. By alloying Mg films with 11.1% of Al or Na, additional charges are distributed over the Mg films. These extra charges contribute to enhance hydrogen binding strength to the films. We focused on the hydrogen affinity of ultrathin Mg films and Mg-Na/Mg-Al thin films. We find that entropic effects including zero point energy contributions have a significant effect on the hydrogen binding. We calculated the Gibbs free energy of the various structures, taking into account the vibrational degrees of freedom. The chemical potentials of hydrogen were evaluated for different types of metal-hydrides. By comparing these with the chemical potential of free hydrogen gas (H_2), we were able to determine the phase boundaries for reversible hydrogen absorption and desorption. We then constructed hydrogenation phase diagrams in P and T space. The formation enthalpies of metal hydrides are greatly increased in thin films, and in stark contrast to its bulk phase, the hydride state can only be stabilized at high P and T, where chemical potential of free H_2 is very high. Therefore, it is necessary to stabilize the thin film structure to some degree. Our study shows that metal doping increases the thermodynamic stabilities of hydride films and significantly helps to reduce the required pressure condition for hydrogen absorption from H_2 gas. In particular, with Na doping hydrogen can be reversibly adsorbed at experimentally accessible T and P conditions.

There are many remaining issues to be addressed for future study. Throughout the paper, we assumed the hcp symmetry and only considered the fcc location for the hydrogen atoms. For solid solutions, one would need to take into account the configurational entropy and interactions between hydrogen atoms. In fact, one should expect phase changes related to the (dis)ordering of dopants and hydrogen atoms, or to the existence of competing crystalline phases. There have been no experiments yet confirming our theoretical predictions of the hydride formation as well as no other theoretical results. In fact, the hydride phase diagram is very complicated and beyond

the scope of this paper. For instance, it is known that the stable hcp phase of bulk Mg changes to a stable rutile MgH_2 structure upon hydrogenation. All in all, the energetics and kinetics of the hydrogenation processes can be very complicated, and it will be necessary to identify the most relevant steps.

All the films considered in this study were free standing films. However, the substrate may also have an important role in stabilizing these films. More importantly to stabilize such a small thickness film, it is very necessary to have a substrate in real systems. Our preliminary studies also indicated that the hydrogen affinity of the films can be altered significantly by applying homogeneous or uniaxial strain to the films [26]. In fact, variations of the hydrogen binding strength via a change of lattice parameters are almost as large as those obtained by changing the film thickness, i.e. thickness and lattice parameters generate similar effects. Further investigations regarding the role of the substrate in growing metal-doped films and their affinity to hydrogen atoms will be pursued.

References

[1] L. Schlapbach and A. Züttel, Nature **414**, 353 (2001).

[2] S. Satyapal *et al.*, Catal. Today **120**, 246 (2007).

[3] I. P. Jain *et al.*, Int. J. Hydrogen Energy **13**, 15 (1988); G. Barkhordarian, T. Klassen, and R. Bormann, J. Phys. Chem. B **110**, 11020 (2006).

[4] J. J. Reilly Jr. and R. H. Wiswall Jr, Inorg. Chem. **7**, 2254 (1968); S. V. Alapati, J. K. Johnson, D. S. Sholl, J. Phys. Chem. B **110**, 8769 (2006).

[5] V. Bérubé *et al*. Int. J. Hydrogen Res. **31**, 637 (2007).

[6] A. Zaluska *et al*., J. Alloys. Comp. **289**, 197 (1999); C. Z. Wu *et al.*, J. Alloys Commp. **420**, 278 (2006); W. Y. Li *et al.*, J. Am. Chem. Soc. **129**, 6710 (2007); X. Yao *et al.*, J. Am. Chem. Soc. **129**, 15650 (2007).

[7] M. M. Ozer, Y. Jia, Z.Y. Zhang, J.R. Thompson, and H.H. Weitering, Science **316**, 1594 (2007).

[8] C.M. Wei and M.Y. Chou, Phys. Rev. B **75**, 195417 (2007).

[9] M. Tallarida, Ph.D. thesis, Freie Univ., 2005.

[10] C. W. Ostenfeld, J. C. Davies, T. Vegge, and I. Chorkendorff, Surf. Sci. **584**, 17 (2005).

[11] K. Higuchi *et al.*, J. Alloys Comp. **293**, 484 (1999); K. Higuchi *et al.*, J. Alloys Comp. **330**, 526 (2002).

[12] X.-G. Li, P. Zhang, and C. K. Chan, Physica B **390**, 225 (2007).

[13] V. Blum, R. Gehrke, F. Hanke, P. Havu, V. Havu, X. Ren, K. Reuter, and M. Scheffler, Comp. Phys. Comm. **180**, 2175 (2009).

[14] V. Havu, V. Blum, P. Havu, and M. Scheffler, J. Comp. Phys. **228**, 8367 (2009).

[15] J. P. Perdew, K. Burke, and M. Ernzerhof, Phys. Rev. Lett. **77**, 3865 (1997).

[16] D. M. Ceperley and B. J. Alder, Phys. Rev. Lett. **45**, 566 (1980); P. Perdew and Y. Wang, Phys. Rev. B **45**, 13244 (1992).

[17] F. D. Murnaghan, PNAS **15**, 244 (1994); F. Birch, Phys. Rev **71**, 809 (1947).

[18] E. Ziambaras and E. Schröder, Phys. Rev. B **68**, 064112 (2003).

[19] C. Kittel, Introduction to Solid State Physics, 6th edition (Wiley, New York, 1986).

[20] D. Errandonea, Y. Meng, D. Häusermann, and T. Uchida, J. Phys.:Condens. Matter **15**, 1277 (2003); H. Olijnyk, J. Phys.: Condens. Matter **16**, 8791 (2004).

[21] M.M. Ozer, C.Z. Wang, Z.Y. Zhang, and H.H. Weitering, J. Low Temp. Phys. **157**, 221 (2009).

[22] F. L. Hirshfeld, Theor. Chim. Acta (Berl.) **44**, 129 (1977).

[23] M. J. Puska, R. M. Nieminen, and M. Manninen, Phys. Rev. B **24**, 3037 (1981).

[24] J. K. Norskov and F. Besenbacher, J. Less Common Met. **130**, 475 (1987).

[25] Y.-L. Liu, Y. Zhang, H.-B. Zhou, G.-H. Lu, F. Liu, G.-N. Luo, Phys. Rev. B **79**, 172103 (2009).

[26] M. W. Chase (Ed.), NIST-JANAF thermochemical tables, 4th edition (American Inst. of Physics, New York, 1998).

[27] K. P. Huber and G. Herzberg, Molecular Spectra and Molecular Structure (Van Nostrand Reinhold Co., 1979).

[28] L. G. Hector, Jr. et al., Phys. Rev. B **76**, 014121 (2007).

[29] K. Reuter and M. Scheffler, Phys. Rev. B **65**, 35406 (2002).

[30] M. Yoon *et al.* (in preparation).

Figure Captions

Figure 1 (Color online). (**a**) Distance distribution function for Mg films, Na_xMg_{1-x}, and Al_xMg_{1-x} alloy films (x=1/9) with thickness τ up to 5 ML (**b**) Distance distribution function for the corresponding metal-hydride films. The structures of the films are fully optimized while maintaining the hcp symmetry. Hydrogen atoms are located at the bulk fcc sites of each film.

Figure 2 (Color online). Partial electron densities of Mg (**a**), Na and Al (**b**), and H (**c**) based on the Hirshfeld analysis. The positive values correspond to the amount of accumulated electrons and negative values for accumulated holes.

Figure 3 (Color online). (**a**) Hydride formation enthalpy (ΔH) of Mg, Na_xMg_{1-x}, and Al_xMg_{1-x} based hydride films (x=1/9) with thickness τ up to 5 ML, where free H_2 gas and (alloyed) film are used as reference systems. At T=0, only the zero point energies contributes to ΔH in addition to the electronic part of the total energies (ΔE). (**b**)-(**d**) Hydrogen chemical potentials ($\Delta\mu_H$) for different metal films, relative to the chemical potential of molecular H_2 at P=1 bar.

Figure 4 (Color online). Hydrogen absorption and desorption phase diagram of Mg films (**a**), NaMg films (**b**), and MgAl films (**c**) in the phase space of temperature and pressure. Each line defines the phase boundary for H-absorption and desorption. Hydrogen absorption is favoured above each line and desorption is favoured below the line. Different colors represent different film thicknesses.
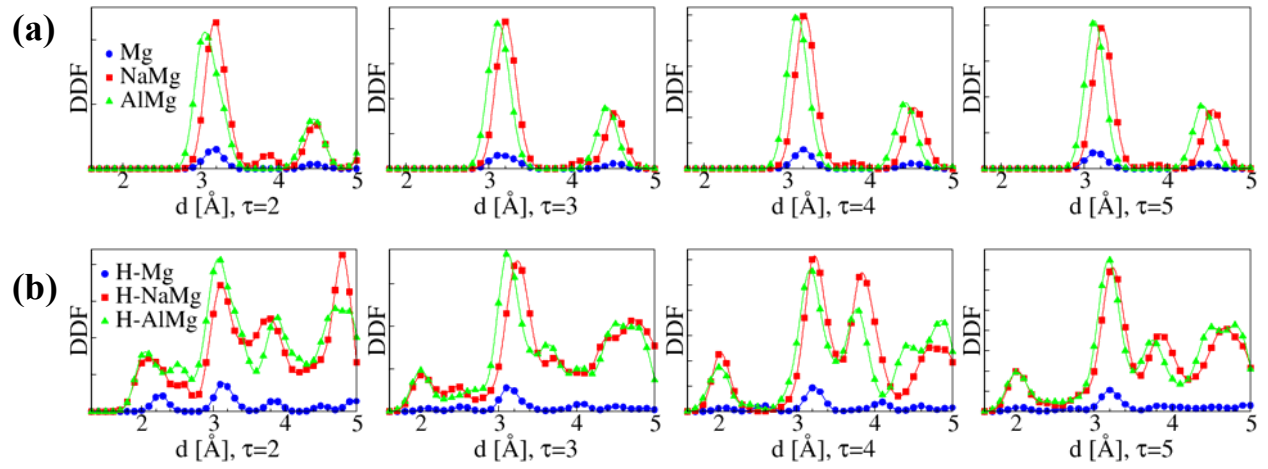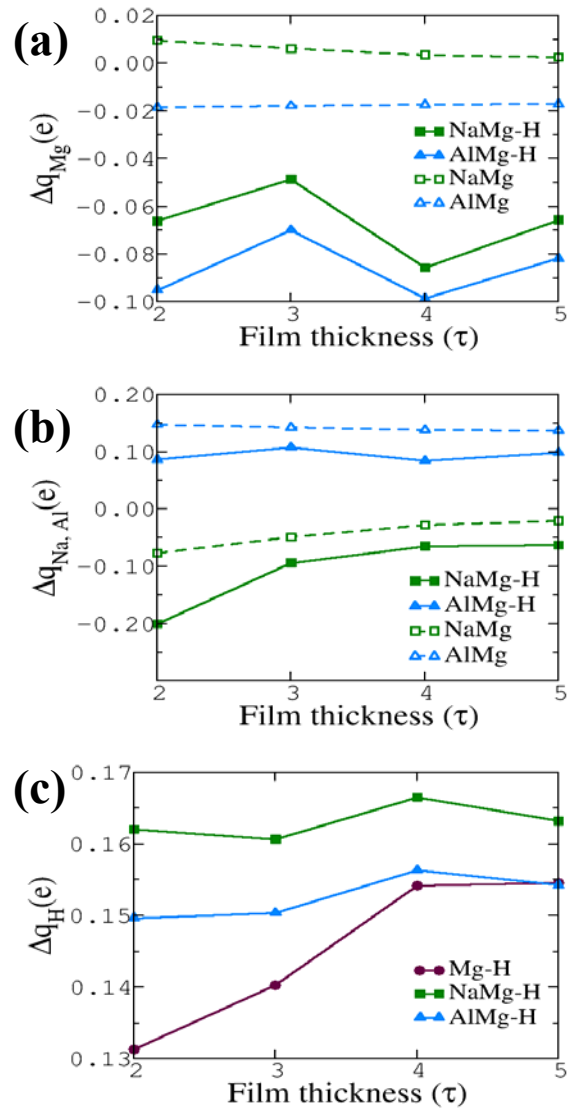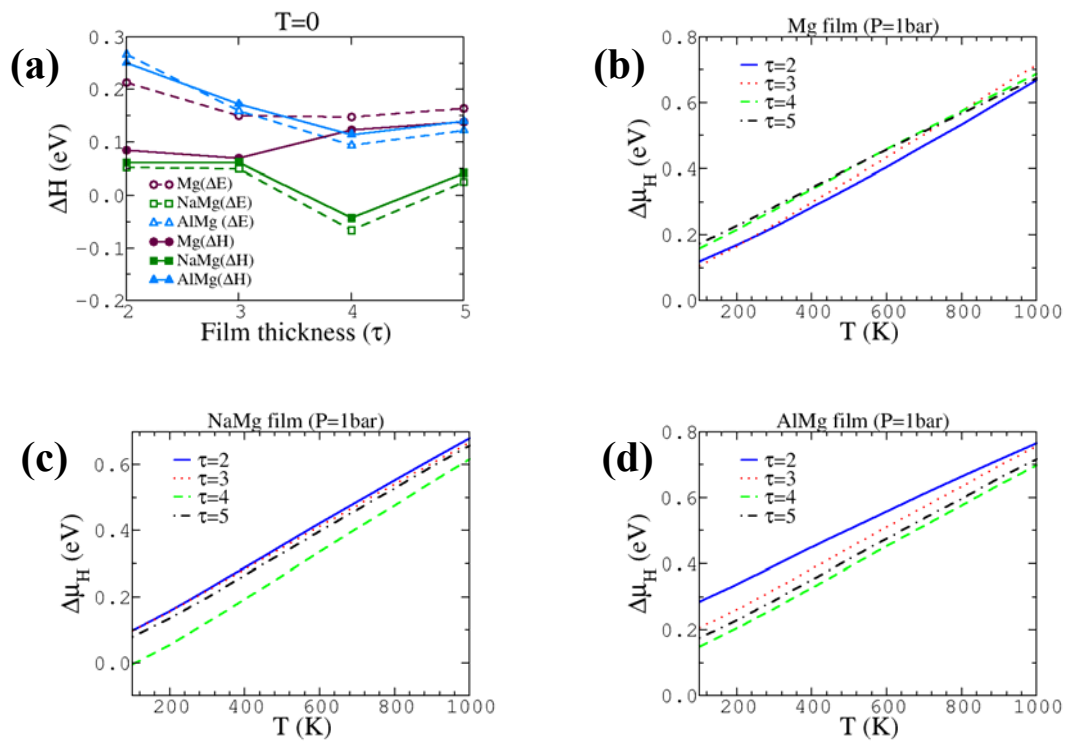
Figure 1

Figure 2
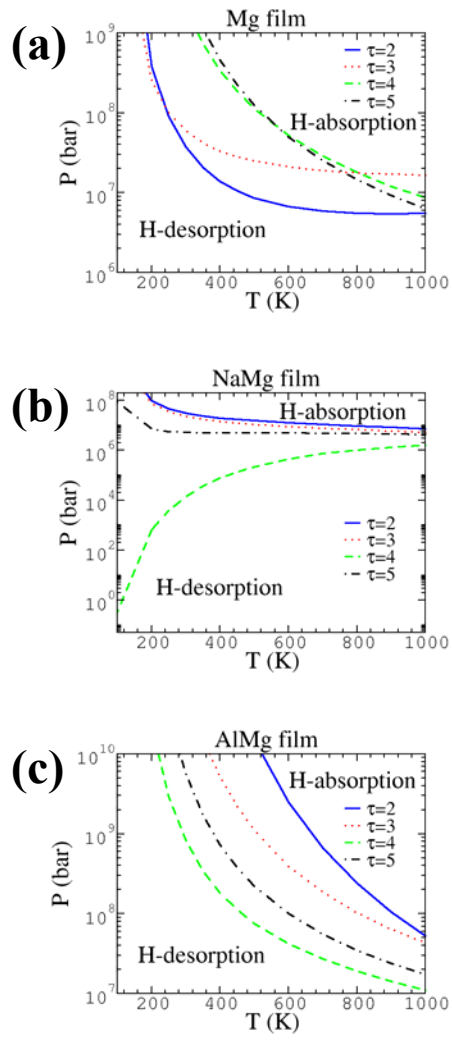
Figure 3

Figure 4